COBEM 2023 27TH INTERNATIONAL CONGRESS OF MECHANICAL ENGENEERING

ABCM Brazilian Society of Mechanical Sciences and Engineering
27th ABCM International Congress of Mechanical Engineering
December 04-08, 2023, Florianópolis-SC, Brazil

COB-2023-0354
PREISACH MODEL APPLIED TO THE THERMOMECHANICAL DESCRIPTION OF SHAPE MEMORY ALLOYS

Thiago Q. Alvares
Vanderson M. Dornelas
Marcelo A. Savi
Center for Nonlinear Mechanics, COPPE - Mechanical Engineering, Universidade Federal do Rio de Janeiro, 21.941.972 Rio de Janeiro, RJ, Brazil
thiagoqa@mecanica.coppe.ufrj.br, vm.dornelas@mecanica.coppe.ufrj.br, savi@mecanica.ufrj.br

Sergio A. Oliveira
Department of Mechanical Engineering, CEFET/RJ – Centro Federal de Educação Tecnológica Celso Suckow da Fonseca, 20.271.110 Rio de Janeiro, RJ, Brazil
sergio.oliveira@cefet-rj.br

Abstract. *Shape memory alloys (SMAs) are adaptive materials that exhibit complex thermomechanical behaviors, including shape memory effect, pseudoelasticity, phase transformation due to temperature variation, internal subloops due to incomplete phase transformation, and tension-compression asymmetry. Due to all these phenomena, the thermomechanical modeling of SMAs is a complex task. Besides, these materials have a significant potential for applications in different areas. Consequently, the modeling of SMAs has scientific and technological relevance. Preisach model is an interesting alternative to describe the SMA hysteretic behavior. This paper presents a numerical investigation of the Preisach model applied to describe the thermomechanical behavior of SMAs. Numerical simulations are carried out to investigate the model capabilities to capture the SMAs behavior. Results are compared with experimental data available in the literature showing to be in close agreement. The Preisach model showed to be an interesting approach since it presents good results combined with a simple numerical implementation when compared to phenomenological and thermodynamic-based models.*

Keywords: *Shape memory alloys, hysteresis, Preisach model, Everett function, numerical simulations.*

1. INTRODUCTION

Shape memory alloys (SMAs) belong to the class of smart materials that have a series of complex thermomechanical behaviors, including shape memory effect, pseudoelasticity, phase transformation due to temperature variation, internal subloops due to incomplete phase transformation, and tension-compression asymmetry. These remarkable properties are attributed to solid-solid martensitic phase transformations (Otsuka and Ren, 2005; Lagoudas, 2008; Yamauchi et al., 2011).

These materials have been employed in applications in various fields, including automotive, biomedical, civil engineering, oil & gas, robotics, and aerospace industries (Machado and Savi, 2003; Mohd Jani et al., 2013; Chang and Araki, 2016; Shreekrishna et al., 2022; Nair and Nachimuthu, 2022). Furthermore, due to their ability to dissipate energy and recover significant deformations during phase transformation, the SMA pseudoelastic behavior offers promising prospects for vibration attenuation. Such applications can be employed in mechanical equipment operating within broad frequency ranges, devices subjected to impact loads, as well as earthquake-resistant structures (Saadat et al., 2002; Leo, 2007; Elahinia, 2016; Vignoli et al., 2020; Silva et al., 2021).

The development of new devices that use SMAs must be associated with the understanding of their thermomechanical properties, in this regard, the modeling of these materials is an essential issue to be considered. A general review of the most relevant models developed in recent years, considering different approaches, is presented by Paiva and Savi (2006), Khandelwal and Buravalla (2009), Cisse et al. (2016a, 2016b), and Chowdhury (2018). The idea of selecting a proper model to describe the different behaviors associated with shape memory alloys is to adapt to the type of approach that can be used.

The Preisach model is a popular model for describing the hysteresis phenomenon (Khandelwal and Buravalla, 2009; Wang et al., 2007). Originally, the classical Preisach model (Preisach, 1935) was developed to describe the behavior of ferromagnetic materials. Only in the 1970s, a new interpretation of the Preisach model was presented by Mark A. Krasnosel'skii and his collaborators (Mayergoyz, 1991). Based on this understanding, the model was able to represent the hysteresis in a general way.

Concerning the hysteresis modeling of shape memory alloys, the Preisach model is associated with some studies in the literature. Smith (2005) presented a discussion of the main points about the use of the Preisach model for modeling shape memory alloys. Hughes and Wen (1995, 1997) listed the microstructural mechanisms that promote hysteresis in SMAs and piezoelectric materials, identifying similarities between hysteresis in these materials and ferromagnetic materials. From this study, the authors concluded that the Preisach model is appropriate to capture the dissipative characteristics of these materials. Gorbet et al. (1998) carried out numerical-experimental comparisons considering the Preisach model, and the experimental results obtained through an actuator composed of SMA wires. Results show that the model responses are in good agreement with experimental data attesting to the model's ability to represent the phenomena associated with SMAs. Mayergoyz (1991, 2003) developed a new formulation of the Preisach model using Everett functions, obtained from experimental data, simplifying the numerical implementation. Khan and Lagoudas (2002) presented a Preisach model based on the formulation proposed by Mayergoyz (1991) to simulate the response of pseudoelastic SMA springs employed in vibration absorbers. In addition, it should be highlighted other studies for instance: Doraiswamy et al. (2011), Rao and Srinivasa (2013), Rao et al. (2014), and Chen et al. (2019).

This paper aims to investigate the use of the Preisach model for the thermomechanical description of shape memory alloys. This model describes the hysteresis from the superposition of operators in a triangular domain, defined in an abstract space, being adjusted from the Everett surface built from experimental data. In this regard, the classic Preisach model is reviewed and a procedure for constructing the Everett function is presented. Numerical simulations are carried out to attest to the model capabilities to describe the SMA thermomechanical behavior. Results are compared with experimental data available in the literature, presenting a good agreement. On this basis, the Preisach model is an interesting approach to describing the thermomechanical behavior of shape memory alloys.

2. MATHEMATICAL MODEL

This Section aims to present a description of the hysteretic behavior of shape memory alloys through the Preisach model. Initially, the Preisach model is discussed and an analysis of its parameters is presented; afterward, the Everett surface is discussed showing its construction from experimental data.

2.1 Preisach model

The Preisach model is built from elementary operators defined in an abstract space, called Preisach hysteresis operators. It is considered that these operators are combined in rectangular loops in an input-output diagram, representing a hysteretic behavior (Mayergoyz, 1991). This operator, $\hat{\gamma}_{\alpha\beta}$, is associated with the abstract variables, α, and β, respectively associated with two directions of transformation, as illustrated in Figure 1. Therefore, when the input is increased, the ascending branch *a-b-c-d-e* is followed. On the other hand, when the input decreases, the descending branch *e-d-f-b-a* is traced. In this regard, a generic hysteresis curve such as stress-strain ($\sigma - \varepsilon$), force-displacement ($f - u$), or strain–temperature ($\varepsilon - T$) can be represented as a sequence of elementary transformations, expressed by the superposition of elementary operations defined by hysteresis operators. Therefore, the hysteresis curve of stress (output), as a function of strain (input), is expressed as follows, assuming that $\alpha \geq \beta$ due to hysteresis being a dissipative phenomenon,

$$\sigma(\varepsilon) = \hat{\Gamma}\varepsilon = \iint_{\alpha \geq \beta} \mu(\alpha, \beta)\, \hat{\gamma}_{\alpha\beta}\, d\alpha\, d\beta \tag{1}$$

where $\mu(\alpha, \beta)$ is the Preisach function, and $\hat{\Gamma}$ represents the Preisach hysteresis operator.

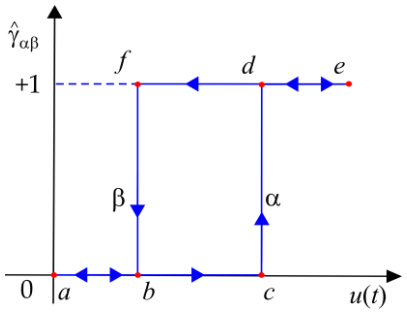

Figure 1. Definition of the Preisach hysteresis operator.

Mayergoyz (1991) reformulates Eq. (1) by replacing integration with a summation of values and the Preisach function with the Everett function (F), constructed from experimental data. This procedure mitigates amplification errors and simplifies the numerical implementation of the model (Khan and Lagoudas, 2002). Therefore, Eq. (1) can be rewritten as a summation of Everett functions:

$$\sigma(\varepsilon) = \sum_{k=1}^{n} [F(\alpha_k, \beta_{k-1}) - F(\alpha_k, \beta_k)] \tag{2}$$

The SMA hysteretic behavior can be predicted using the Preisach model following the structure illustrated in Figure 2. Experimental data are used to build the Everett surface that allows one to establish the relationship with the Preisach space, where the SMA description is possible.

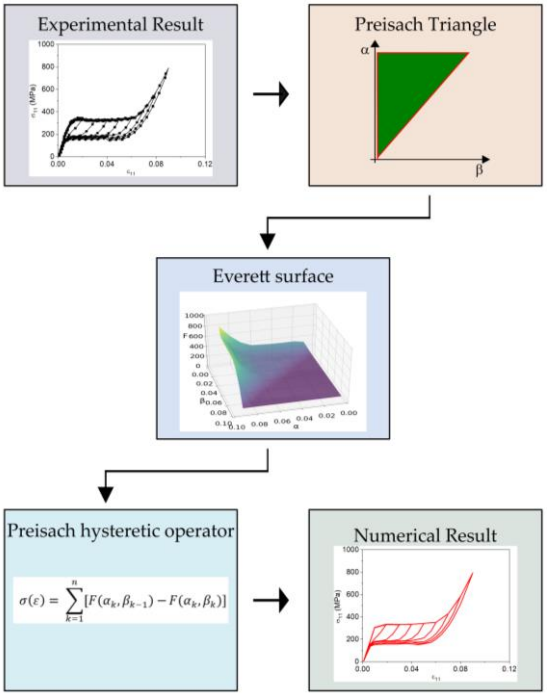

Figure 2. Application scheme of the SMA Preisach model.

2.2 Geometric Interpretation

The geometric interpretation of the Preisach triangle is shown in Figure 3 considering a stress-strain curve. In this regard, the triangular representation is constructed considering that the upper limit in α coordinate corresponds to the maximum strain value. On the other hand, the lower limit in the β coordinate corresponds to the minimum strain value. The line $\alpha = \beta$ is added to these limits, considering $\alpha \geq \beta$. In addition, considering the example illustrated in Figure 3, the stress value at any point in the hysteresis region can be obtained from the appropriate choice of $\alpha - \beta$ coordinates, followed by the construction of the Everett function.

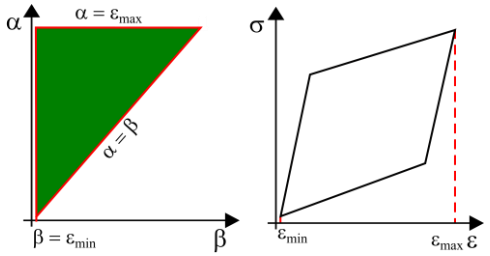

Figure 3. Preisach triangle and the associated hysteresis.

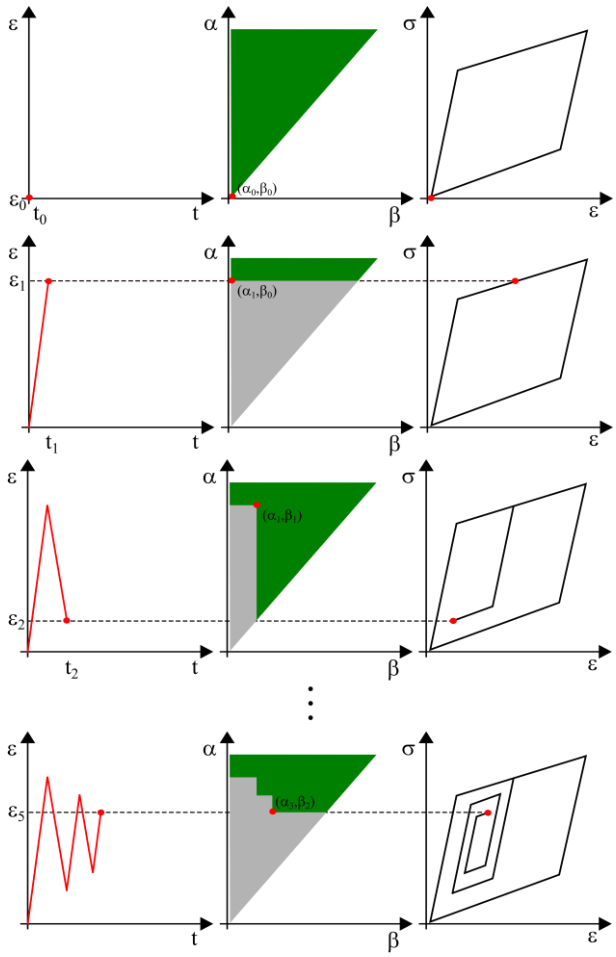

Figure 4. Evolution of the Preisach triangle and the associated hysteresis obtained considering a prescribed strain.

The representation of the hysteresis evolution in the Preisach triangle is schematically shown in Figure 4. In general, an increase in the value of ε provides a change in the α-axis while a decrease changes the β-axis. Furthermore, an increase in the value of ε implies summing a value of the Everett function in Eq. (2) and a decrease of ε implies subtracting a value from the Everett function in Eq. (2).

On this basis, at the initial time, t_0, the material has a strain ε_0 at the beginning of the hysteresis region. At this moment, the coordinates in the Preisach plane are $(\alpha_0, \beta_0) = (\varepsilon_0, \varepsilon_0)$. After identifying the coordinates in the Preisach plane, the Everett surface is calculated and applied in Eq. (2) obtaining the stress value of $\sigma(\varepsilon) = F(\alpha_0, \beta_0)$. After that, the strain increases continuously until it reaches a value ε_1. The variation of strain is represented by the grayscale color in the Preisach triangle. The division is performed by the line $\alpha = \varepsilon$, which moves upward as ε increases until it reaches ε_1. Since this is the first variation in the α coordinate, it is labeled with the index 1. Thus, the new coordinates in the Preisach plane are obtained, $(\alpha_1, \beta_0) = (\varepsilon_1, \varepsilon_0)$, and the Everett function is determined. Appling Eq. (2) the value of the stress is calculated as $\sigma(\varepsilon) = F(\alpha_1, \beta_0)$. The Preisach model has the property of capturing only the extreme points of the α and β coordinates (Mayergoyz, 1991), in this sense, an increment in the α coordinate represents the replacement of the Everett function $F(\alpha_0, \beta_0)$ by $F(\alpha_1, \beta_0)$.

In the sequence, it is assumed that the input variable decreases continuously until it reaches a minimum value ε_2. The boundary line shown in the Preisach triangle now has two straight lines: one horizontal and one vertical. The vertical line moves until it reaches $\beta = \varepsilon_2$. Because it is the first variation in the beta coordinate, it receives the index 1. Once again, applying the coordinates obtained in the Preisach plane $(\alpha_1, \beta_1) = (\varepsilon_1, \varepsilon_2)$, the Everett function is determined. Therefore, the stress value can be obtained through Eq. (2) and is written as: $\sigma(\varepsilon) = F(\alpha_1, \beta_0) - F(\alpha_1, \beta_1)$. This result illustrates another property of the Preisach model, which consists of accumulating the values obtained in previous operations. Note that $\sigma(\varepsilon)$ is composed of a portion obtained in the previous step accumulated with the result obtained in the current step as defined in Eq. (2).

2.3 Everett function

The Everett function is a surface on $\Re^3$, built from experimental data and establishing a connection with the Preisach domain. The Everett surface is obtained by defining the number of experimental points necessary for the description of the hysteretic behavior, given through the coordinate points (α, β, F) in the region of the Preisach triangle. After that, a two-dimensional linear interpolation is performed, defining the Everett function. Figure 5 illustrates the steps for obtaining the Everett surface by dividing the stress-strain space into nine regions. The experimental points identified in the stress-strain curve are highlighted by red dots, shown in Figure 5(a). The Preisach triangle obtained through the experimental points is illustrated in Figure 5(b). The points identified in red are the points on the Preisach triangle plane $(\alpha \geq \beta)$. Furthermore, the mapped experimental points are represented in the Preisach triangle as solid points. On the other hand, the points identified in gray color represent the external points to the Preisach triangle. Finally, Figure 5(c) shows the Everett surface obtained considering the mapped experimental points. It is observed from this example that the Everett function appears as an envelope of the region of the Preisach triangle (solid red dots).

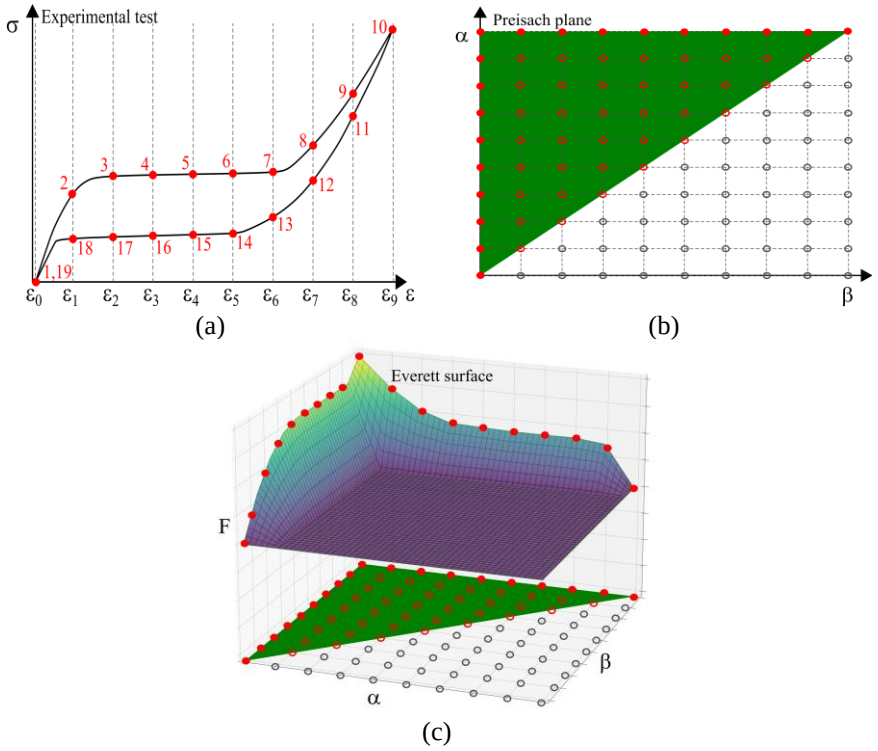

Figure 5. Everett surface construction. (a) Experimental points mapped from a division of the hysteresis region; (b) associated Preisach triangle considering the mesh obtained from the proposed division; (c) Everett surface obtained.

A procedure to determine the coordinate points (α, β, F), is presented in the sequel:

1. Select the experimental data.
2. Divide the hysteresis region into an appropriate number of divisions using vertical lines.
3. Identify the experimental points obtained by the intersection between the vertical lines and the experimental data.
4. Identify the experimental strain values to obtain α and β values.
5. Build the $H_{\alpha\beta}$ stress matrix, which defines the third coordinate to obtain the Everett surface.
6. Build the Everett function by two-dimensional linear interpolation.

In order to illustrate the procedure for obtaining the $H_{\alpha\beta}$ matrix, consider the experimental data shown in Figure 5(a) with nine divisions of the stress-strain space. From lines $\varepsilon_{0\to9}$, nineteen experimental points are obtained as shown in Table 1. It is observed that points 1 and 19 are coincident, and therefore, present the same strain and stress.

There is correspondence between the stress-strain space and the Preisach domain. Therefore, it is necessary to map the Preisach plane for the ten lines $\varepsilon_{0\to9}$, considering $\alpha_i = \beta_i = \varepsilon_i$ (i varying between 0 and 9) as illustrated in Figure 5(b). These coordinates are identified in Table 2.

Table 1. Experimental points obtained by dividing the stress-strain space into nine regions.

Experimental point	Strain	Stress
1	ε_0	σ_1
2	ε_1	σ_2
⋮	⋮	⋮
9	ε_8	σ_9
10	ε_9	σ_{10}
11	ε_8	σ_{11}
⋮	⋮	⋮
18	ε_1	σ_{18}
19	ε_0	$\sigma_{19} = \sigma_1$

The third coordinate F is obtained through the stress matrix $H_{\alpha\beta}$, where α and β are the columns and rows of this matrix, respectively. The matrix $H_{\alpha\beta}$ has only the first row and the last column with values different from zero. The construction of this matrix is illustrated in Table 2. The values of the first line are found by subtracting the smallest stress value of the experimental points of the austenite → martensite transformation (σ_1) from the stress values of each experimental point of this same transformation ($\sigma_1 - \sigma_{10}$). On the other hand, the values in the last column are obtained by subtracting the highest stress value of the experimental points of the martensite → austenite transformation (σ_{10}) from the stress values of each experimental point of this transformation ($\sigma_{19} - \sigma_{10}$). After obtaining the $H_{\alpha\beta}$ matrix, a two-dimensional linear interpolation of the points is performed and the Everett surface is obtained, as shown in Figure 5(c).

Table 2. Determination of the $H_{\alpha\beta}$ matrix.

	α_0	α_1	...	α_8	α_9
β_0	$\sigma_1 - \sigma_1$	$\sigma_2 - \sigma_1$	...	$\sigma_9 - \sigma_1$	$\sigma_{10} - \sigma_1$
β_1	0	0	...	0	$\sigma_{10} - \sigma_{18}$
⋮	⋮	⋮	⋱	⋮	⋮
β_8	0	0	...	0	$\sigma_{10} - \sigma_{11}$
β_9	0	0	...	0	$\sigma_{10} - \sigma_{10}$

3. NUMERICAL RESULTS

Numerical simulations are now carried out in order to show the Preisach model's capabilities to describe the thermomechanical behavior of SMAs. In this regard, comparisons between numerical and experimental results available in the literature are discussed. Basically, three situations are of concern: thermal loading; helical springs subjected to tensile loading; helical springs subjected to tensile-compression loading.

3.1 Thermal Loading

The thermomechanical behavior of shape memory alloys due to thermal loadings is now in focus considering the experimental result presented by Qin et al. (2019) as reference. In this work, the authors studied the structural and functional fatigue of NiTi wires subjected to different thermal loads, initially in the austenitic phase, at constant stress. Figure 6(a) shows the experimental strain-temperature curve obtained after ten training cycles varying the sample temperature between 367-292 K and the respective selected experimental points, with which the Everett function is constructed considering nine divisions. It should be pointed out that temperature is the input variable and strain is the output. Since the increase in temperature causes a decrease in the strain, the Preisach triangle is adjusted as shown in Figure 6(b). Since only experimental points from the outer loop are available, the Everett function is just the envelope of the Preisach triangle illustrated in Figure 6(c). Figure 6(d) presents the comparison between numerical and experimental results showing that the Preisach model captures the general behavior observed in experimental data, presenting a good agreement.

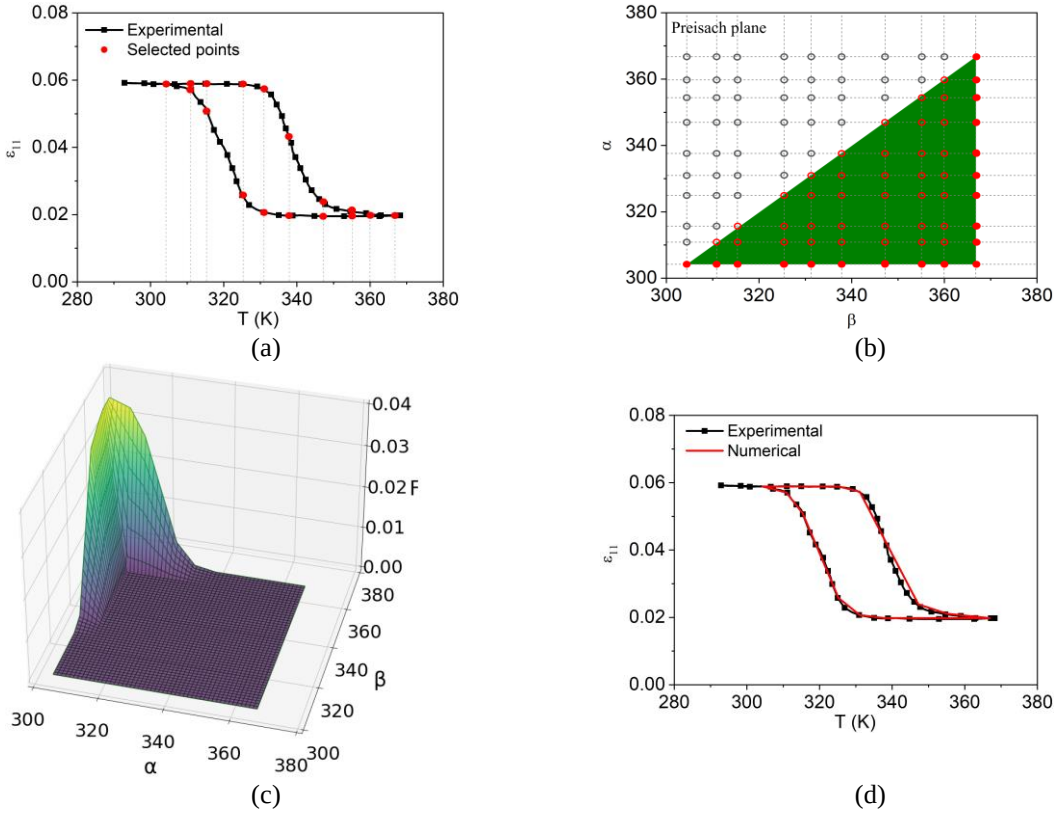

Figure 6. Thermal cyclic test under a constant uniaxial load based on the experimental test due to Qin et al. (2019). (a) experimental curve; (b) Preisach triangle; (c) Everett surface; (d) numerical-experimental comparison.

3.2 Helical Spring Subjected to Tensile Loading

The Preisach model is now employed to analyze the macroscopic behavior of a NiTi helical spring subjected to tensile tests considering the experimental result presented by Savi et al. (2015). Figure 7(a) shows the experimental force-displacement curve divided into nine regions and the respective points selected for the numerical implementation of the Everett function. Figure 7(b) shows the associated Preisach triangle. Again, the Everett function appears as an envelope of the Preisach triangle region since only experimental points of the outer loop are considered, as shown in Figure 7(c). Figure 7(d) presents the numerical-experimental comparison where it should be pointed out a good agreement between results. It is noticeable that the Preisach model is capable to describe the pseudoelastic behavior of SMA springs.

3.3 Helical Spring Subjected to Tensile-Compression Loading

The Preisach model is now employed to analyze the tension-compression asymmetry of a NiTi helical spring considering the experimental test proposed by Speicher et al. (2009) as a reference. Figure 8(a) shows the experimental result, highlighting the proposed divisions and the experimental points. Figure 8(b) shows the Preisach triangles associated with both tension and compression. It is possible to observe in Figure 8(b) the blue region that represents the domain in which the Everett function corresponds to the linear region connecting the hysteresis cycles of tension and compression. Once again, only the experimental data of the external loops are considered, and the Everett function is an envelope of the Preisach triangles shown in Figure 8(c). Finally, Figure 8(d) shows the numerical-experimental comparison. It should be pointed out the good agreement between numerical and experimental results, showing the model's capability to represent the tension-compression asymmetry of the SMA springs.

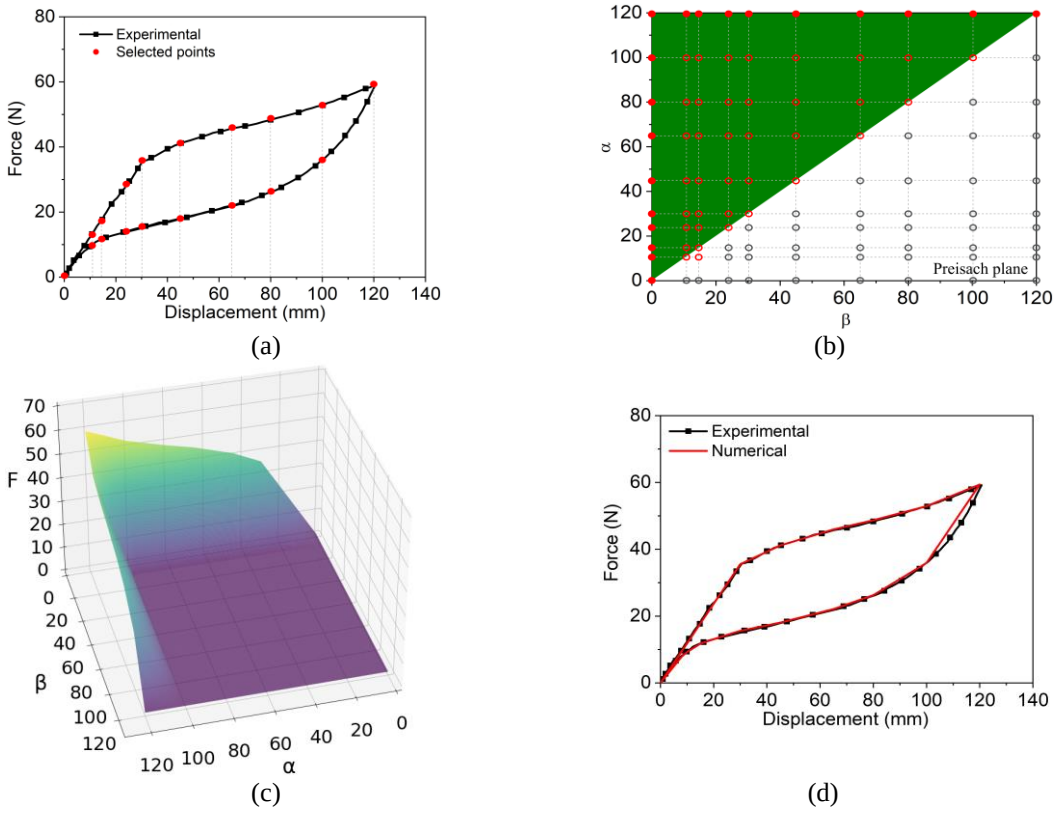

Figure 7. Numerical-experimental force-displacement curves based on the experimental test due to Savi et al. (2015). (a) experimental curve; (b) Preisach triangle; (c) Everett surface; (d) numerical-experimental comparison.

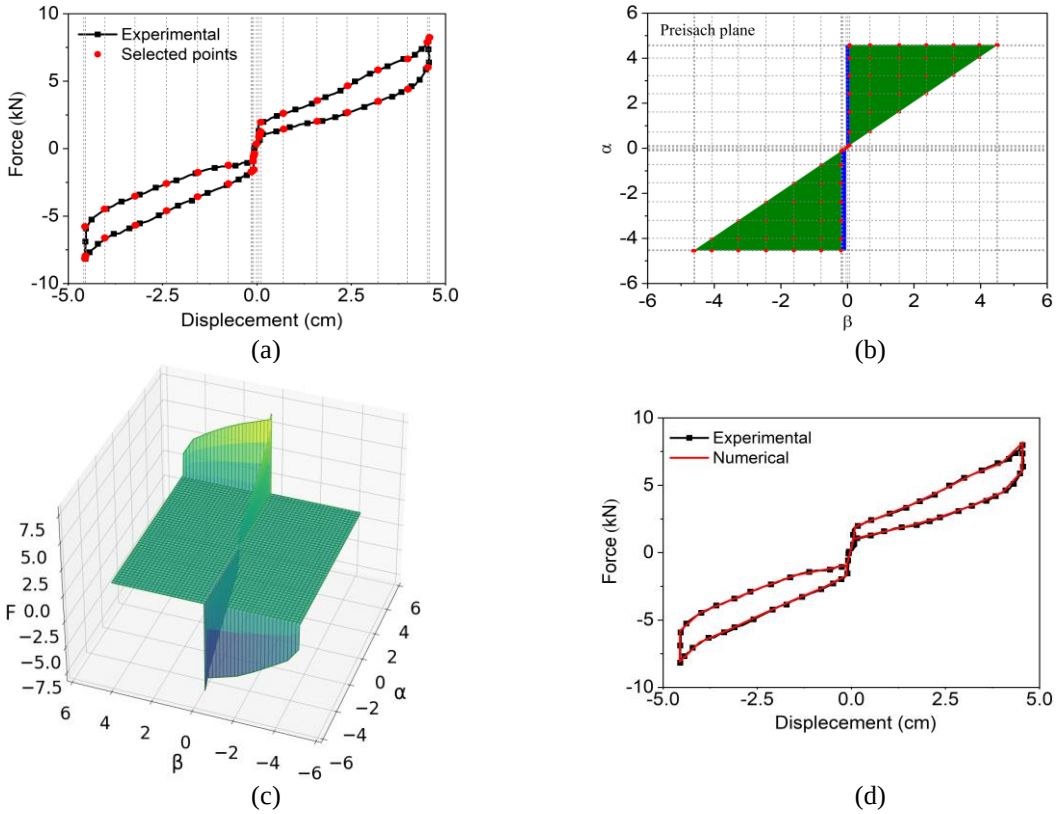

Figure 8. Numerical-experimental force-displacement curves based on the experimental test due to Speicher et al. (2009). (a) experimental curve; (b) Preisach triangle; (c) Everett surface; (d) numerical-experimental comparison.

4. CONCLUSIONS

This contribution presents a numerical investigation of the thermomechanical behavior of shape memory alloys from the Preisach model. The model is able to capture the main features of the SMA thermomechanical behavior, properly describing stress-strain, force-displacement or strain-temperature curves. The Preisach model employs the Everett function that, in turn, is built from experimental data. Numerical results are compared with experimental data available in the literature considering three different tests: thermal loads, tensile loads, and tensile-compression loads. Results show that the model responses are in close agreement with experimental data.

5. ACKNOWLEDGEMENTS

The authors would like to acknowledge the support of the Brazilian Research Agencies FAPERJ, CNPq, and CAPES.

6. REFERENCES

Chang, W.S. and Araki, Y., 2016. "Use of shape-memory alloys in construction: A critical interview". In *Proceedings of the Institution of Civil Engineers-Civil Engineering 2016*, Vol. 169, No. 2, pp. 87–95.

Chen, Y., Shen, X., Li, J., Chen, J., 2019. "Nonlinear hysteresis identification and compensation based on the discrete Preisach model of an aircraft morphing wing device manipulated by an SMA actuator". *Chinese Journal of Aeronautics*, Vol. 32, No. 4, pp. 1040–1050.

Cisse, C., Zaki, W., Zineb, T.B., 2016a. "A review of constitutive models and modeling techniques for shape memory alloys". *International Journal of Plasticity*, Vol. 76, pp. 244–284.

Cisse, C., Zaki, W., Zineb, T.B., 2016b. "A review of modeling techniques for advanced effects in shape memory alloy behavior". *Smart Materials and Structures*, Vol. 25, pp. 103001.

Chowdhury, P., 2018. "Frontiers of theoretical research on shape memory alloys: A general overview". *Shape Memory and Superelasticity*, Vol. 4, pp. 26–40.

Doraiswamy, S., Rao, A., Srinivasa, A.R., 2011. "Combining thermodynamic principles with Preisach models for superelastic shape memory alloy wires". *Smart Materials and Structures*, Vol. 20, No. 8, pp. 085032.

Elahinia, MH. *Shape memory alloy actuators: design, fabrication, and experimental evaluation*. John Wiley & Sons Ltd: New York.

Gorbet, R.B., Wang, D.W., Morris, K.A., 1998. "Preisach model identification of a two-wire SMA actuator". In *Proceedings. 1998 IEEE International Conference on Robotics and Automation*, Vol. 3, pp. 2161–2167.

Hughes, D.C. and Wen, J.T., 1995. "Preisach modeling and compensation for smart material hysteresis". In: *Active materials and smart structures. SPIE*, Vol. 2427, pp. 50–64.

Hughes, D.C. and Wen, J.T., 1997. "Preisach modeling of piezoceramic and shape memory alloy hysteresis". *Smart materials and structures*, Vol. 6, No. 3, pp. 287.

Khan, M.M. and Lagoudas, D.C., 2002. "Modeling of shape memory alloy pseudoelastic spring elements using Preisach model for passive vibration isolation". In *Smart Structures and Materials 2002: Modeling, Signal Processing, and Control SPIE*, Vol. 4693, pp. 336–347.

Khandelwal, A. and Buravalla, V., 2009. "Models for shape memory alloy behavior: an overview of modeling approaches". *The International Journal of Structural Changes in Solids*, Vol. 1, No. 1, pp. 111–148.

Lagoudas, D.C., 2008. *Shape Memory Alloys, Modeling and Engineering Applications*. Springer: Austin, TX, USA.

Leo, D.J., 2007. *Engineering analysis of smart material systems*. John Wiley and Sons: New Jersey.

Machado, L.G. and Savi, M.A., 2003. "Medical applications of shape memory alloys". *Brazilian Journal of Medical and Biological Research*. Vol. 36, No. 6, pp. 683–691.

Mohd Jani, J., Leary, M., Subic, A., Gibson, M.A., 2013. "A review of shape memory alloy research, applications and opportunities". *Materials & Design*, Vol. 56, pp. 1078–1113.

Otsuka, K. and Ren, X., 2005. "Physical metallurgy of TiNi based shape memory alloys". *Progress in materials science*, Vol. 50, No. 5, pp. 511–678.

Mayergoyz, I.D., 1991. *Mathematical Models of Hysteresis.* Springer Verlag: New York.

Mayergoyz, I.D., 2003. *Mathematical models of hysteresis and their applications*. College Park, USA, Academic Press.

Nair, V.S., Nachimuthu, R., 2022. "The role of NiTi shape memory alloys in quality of life improvement through medical advancements: A comprehensive review". In *Proceedings of the Institution of Mechanical Engineers, Part H: Journal of Engineering in Medicine*, Vol. 236, No. 7, pp. 923–950.

Paiva, A. and Savi, M.A., 2006. "An Overview of constitutive models for shape memory alloys". *Mathematical problems in engineering*, pp. 1–30.

Preisach, F. "Über die magnetische Nachwirkung". *Zeitschrift für physik*, Vol. 94, pp. 277–302.

Qin, X., Zhang, X., Yan, X., Wang, S., Zhang, S., Guo, C., Jiang, J., Zhang, B., Huang, D., Qi, M., 2019. "Structural and functional fatigue behavior of Ni49.8Ti50.2 (at. %) wires under various maximum heating temperatures: Experimental and modeling study". *Materials & Design*, Vol. 178, pp. 107842.

Rao, A. and Srinivasa, A.R., 2013. "A two-species thermodynamic Preisach model for the torsional response of shape memory alloy wires and springs under superelastic conditions". *International Journal of Solids and Structures*, Vol. 50, No. 6, pp. 887–898.

Rao, A., Ruimi, A., Srinivasa, A. R., 2014. "Internal loops in superelastic shape memory alloy wires under torsion-experiments and simulations/predictions. *International Journal of Solids and Structures*, Vol. 51, No. 25–26, pp. 4554–4571.

Saadat, S., Salichs, J., Noori, M., Hou, Z., Davoodi, H., Baron, I., Suzuki, Y., Masuda, A., 2002. "An overview of vibration and seismic applications of NiTi shape memory alloy". *Smart materials and structures*, Vol. 11, No. 2, pp. 218.

Savi, M.A., Pacheco, P.M.C., Garcia, M.S., Aguiar, R.A., De Souza, L.F.G., Da Hora, R.B., 2015. "Nonlinear geometric influence on the mechanical behavior of shape memory alloy helical springs". ". *Smart Materials and Structures*, Vol. 24, No. 3, pp. 035012.

Shreekrishna, S., Nachimuthu, R., Nair, V.S., 2022. "A review on shape memory alloys and their prominence in automotive technology". *Journal of Intelligent Material Systems and Structures*, pp. 1–26.

Silva, R.S., Ritto, T.G., Savi, M.A., 2021. "Shape memory alloy couplers applied for torsional vibration attenuation of drill-string systems". *Journal of Petroleum Science and Engineering*, Vol. 202, pp. 108546.

Smith, R.C., 2005. *Smart Material Systems: Model development*. Society for Industrial and Applied Mathematics, 2005, SIAM, USA.

Speicher, M., Hodgson, D.E., DesRoches, R., Leon, R.T., 2009. "Shape memory alloy tension/compression device for seismic retrofit of buildings*". Journal of Materials Engineering and Performance*, Vol. 18, pp. 746-753.

Vignoli, L.L., Savi, M.A., El-Borgi, S., 2020. "Nonlinear dynamics of earthquake-resistant structures using shape memory alloy composites". *Journal of Intelligent Material Systems and Structures*., Vol. 31, No. 5, pp. 771–787.

Wang, Y.F., Su, C.Y., Hong, H., Hu, Y.M., 2007. "Modeling and compensation for hysteresis of shape memory alloy actuators with the Preisach representation". In *2007 IEEE international conference on Control and Automation*, pp. 239–244.

Yamauchi, K., Ohkata, I., Tsuchiya, K., Miyazaki, S., 2011. *Shape memory and superelastic alloys: Applications and technologies*. Woodhead Publishing: Cambridge, U.K.

7. RESPONSIBILITY NOTICE

The authors are the only responsible for the printed material included in this paper.